Remote Sensing of Environment 240 (2020) 111696

Contents lists available at ScienceDirect

Remote Sensing of Environment

journal homepage: www.elsevier.com/locate/rse

A voxel matching method for effective leaf area index estimation in temperate deciduous forests from leaf-on and leaf-off airborne LiDAR data

Xi Zhu[a,*], Jing Liu[a,b,c], Andrew K. Skidmore[a,d], Joe Premier[e], Marco Heurich[e,f]

[a] Faculty of Geo-Information Science and Earth Observation (ITC), University of Twente, P.O. Box 217, 7500, AE, Enschede, the Netherlands
[b] Key Laboratory of Virtual Geographic Environment, Ministry of Education, Nanjing Normal University, Nanjing 210023, China
[c] School of Geography, Nanjing Normal University, Nanjing 210023, China
[d] Department of Environmental Science, Macquarie University, NSW 2109, Australia
[e] Bavarian Forest National Park, Freyunger Straße 2, 94481 Grafenau, Germany
[f] Chair of Wildlife Ecology and Management, Faculty of Environment and Natural Resources, University of Freiburg, Freiburg, Germany

ARTICLE INFO

Keywords:
Effective leaf area index
Airborne LiDAR
Leaf-off
Leaf-on
Voxel matching

ABSTRACT

The quantification of leaf area index (LAI) is essential for modeling the interaction between atmosphere and biosphere. The airborne LiDAR has emerged as an effective tool for mapping plant area index (PAI) in a landscape consisting of both woody and leaf materials. However, the discrimination between woody and leaf materials and the estimation of effective LAI (eLAI) have, to date, rarely been studied at landscape scale. We applied a voxel matching algorithm to estimate eLAI of deciduous forests using simulated and field LiDAR data under leaf-on and leaf-off conditions. We classified LiDAR points as either a leaf or a woody hit on leaf-on LiDAR data by matching the point with leaf-off data. We compared the eLAI result of our voxel matching algorithm against the subtraction method, where the leaf-off effective woody area index (eWAI) is subtracted from the effective leaf-on PAI (ePAI). Our results, which were validated against terrestrial LiDAR derived eLAI, showed that the voxel matching method, with an optimal voxel size of 0.1 m, produced an unbiased estimation of terrestrial LiDAR derived eLAI with an R^2 of 0.70 and an RMSE of 0.41 (RRMSE: 20.1%). The subtraction method, however, yielded an R^2 of 0.62 and an RMSE of 1.02 (RRMSE: 50.1%) with a significant underestimation of 0.94. Reassuringly, the same outcome was observed using a simulated dataset. In addition, we evaluated the performance of 96 LiDAR metrics under leaf-on conditions for eLAI prediction using a statistical model. Based on the importance scores derived from the random forest regression, nine of the 96 leaf-on LiDAR metrics were selected. Cross-validation showed that eLAI could be predicted using these metrics under leaf-on conditions with an R^2 of 0.73 and an RMSE of 0.27 (RRMSE: 17.4%). The voxel matching method yielded a slightly lower accuracy (R^2: 0.70, RMSE:0.41, RRMSE: 20.1%) than the statistical model. We, therefore, suggest that the voxel matching method offers a new opportunity for the estimating eLAI and other ecological applications that require the classification between leaf and woody materials using airborne LiDAR data. It potentially allows transferability to different sites and flight campaigns.

1. Introduction

Leaf area index (LAI) is typically defined as one-sided leaf area per unit ground surface area (Chen and Black, 1992), and numerous direct and indirect techniques have been developed for the rapid and regular estimation of LAI (Neumann et al., 1989; Wilson, 1963). LAI is a key canopy structural parameter that impacts on the exchange of gas, energy and mass between the biosphere and atmosphere (Gobron et al., 1997). It determines ecosystem functioning (Bonan, 1995; Bonan, 2015; Rautiainen, 2005) and drives many biological and physical processes, such as photosynthesis, transpiration, light and rainfall interception as well as the carbon cycle (Asrar et al., 1984; Cattanio, 2017; Chen and Cihlar, 1996; Hardwick et al., 2015; Tian et al., 2015). Due to its important role in these processes, LAI has been selected as an essential biodiversity variable (Pettorelli et al., 2016; Skidmore et al., 2015), and has been widely used in ecological and climate models (Roy et al., 2012; Xiao and McPherson, 2002).

Directly measuring LAI is the most accurate method of estimation, but pragmatically limited to small areas as the field work is time consuming, tedious, and destructive to vegetation where leaf harvesting is

* Corresponding author.
E-mail address: x.zhu@utwente.nl (X. Zhu).

https://doi.org/10.1016/j.rse.2020.111696
Received 26 September 2019; Received in revised form 10 January 2020; Accepted 30 January 2020

employed (Jonckheere et al., 2004). *In-situ* indirect techniques using optical instruments such as LI-COR LAI-2000, TRAC or digital hemispherical photography (DHP) have been proposed to replace direct measurement (Chen and Cihlar, 1995; Leblanc et al., 2002). Over the years these optical instruments have proven useful for *in-situ* measurement and validation (Weiss et al., 2004), but do not provide clear separation between leaf and woody materials, since the radiometric information is affected by light and shadow conditions within a forest (Jonckheere et al., 2004). The derived LAI quoted in many studies is in fact plant area index (PAI), consisting of both woody and leaf materials (Luo et al., 2015; Tillack et al., 2014). To actually measure LAI instead of PAI, a suitable alternative can be the use of LiDAR (discrete light detection and ranging) data (Béland et al., 2014; Calders et al., 2018). LiDAR data of a forest canopy contain three-dimensional (3D) information, and have been widely used to estimate various forest canopy structural parameters (Farid et al., 2008; Hopkinson and Chasmer, 2009; Ma et al., 2017).

Terrestrial LiDAR also referred to as terrestrial laser scanning (TLS), provides highly detailed structural canopy information thanks to its fine angular resolution and close range (Zhao et al., 2011). Various methods for obtaining LAI from terrestrial LiDAR data have been proposed and proven accurate (Béland et al., 2014; Hancock et al., 2014; Hosoi and Omasa, 2006). Consequently, it has been recognized as a good ground validation technique for remote sensing (Hancock et al., 2017; Oshio et al., 2015). In addition, the classification between leaf and woody components using terrestrial LiDAR has also been well studied and good classification accuracy has been achieved in recent years (Béland et al., 2011; Ma et al., 2017; Zheng et al., 2016; Zhu et al., 2018). (Ma et al., 2016b) developed a classification method to separate leaf and woody components using terrestrial LiDAR data, obtaining an overall accuracy of 93.1% for coniferous trees and 95.5% for broadleaf trees. An adaptive radius near-neighbor search approach was proposed by (Zhu et al., 2018) for feature derivation to separate foliar and woody materials, achieving an average overall accuracy of 84.4% for mixed forests on variable slopes and with mixed understory cover.

Airborne LiDAR also known as airborne laser scanning (ALS), provides precise 3D coordinates of the object as well as backscatter intensity for each measured point at large scales (Kashani et al., 2015). Airborne LiDAR has been widely used for forest applications, especially the evaluation of 3D forest structure (Bouvier et al., 2015; Pearse et al., 2017; Sumnall et al., 2017). LAI, as one of the most important forest structure variables, has been linked to the penetration ratio of laser pulses using airborne LiDAR techniques. These approaches usually consider the ratio of the number of returns below the canopy to the total number of returns, and link this ratio to an estimate of the transmittance or gap fraction of the canopy (Hopkinson et al., 2013; Solberg et al., 2009). Subsequently, LAI can be estimated using the Beer-Lambert Law that converts gap fraction to LAI (Chen, 1996; Nilson, 1971). Due to the lower point density and bigger footprint of airborne LiDAR data relative to terrestrial LiDAR data, the classification between leaf and woody components used in terrestrial LiDAR data is not applicable to airborne LiDAR data. Geometric features require very high point densities to show the spatial pattern of a single leaf or a small branch. Moreover, due to this relatively large footprint of airborne LiDAR data, the radiometric features (*e.g.* intensity) are not easy to interpret, since the returned energy from the canopy is often an interaction between the transmitted pulse and multiple targets. Consequently, LAI estimated from airborne LiDAR data usually actually represents effective PAI (ePAI), *i.e.* without the woody contribution having been removed (Alonzo et al., 2015; Tang et al., 2014).

Some previous studies have used leaf-on and leaf-off airborne LiDAR data for forest applications. The study of (Næsset, 2005) evaluated LiDAR metrics derived from both leaf-on and leaf-off data for forest canopy height measures. (Hill and Broughton, 2009) examined the understory information using airborne LiDAR data acquired in both leaf-on and leaf-off conditions. (Kim et al., 2009) tested leaf-on and leaf-off LiDAR intensity for tree species classification and demonstrated the potential of combining two datasets. (Parent and Volin, 2014) assessed the potential of leaf-off airborne LiDAR data to model canopy closure. However, to the best of our knowledge, no researcher has evaluated the use of temporally consecutive leaf-on and leaf-off airborne LiDAR data to discriminate LAI and woody area index (WAI) from PAI.

Although the joint use of leaf-on and leaf-off airborne LiDAR data has not been applied for LAI estimation, theories and approaches have been developed and evaluated for the estimation of LAI and WAI for leaf-on and leaf-off terrestrial LiDAR data. (Béland et al., 2011) examined the differences of intensity between leaf and woody components using leaf-on and leaf-off terrestrial LiDAR data, and found an optimal threshold for the classification. (Li et al., 2016) directly separated woody points in leaf-off data from leaf points in leaf-on data using terrestrial LiDAR data. Recently, (Calders et al., 2018) estimated effective WAI (eWAI) in leaf-off conditions as well as ePAI in leaf-on conditions, and obtained eLAI by subtracting eWAI from ePAI, indicating a strong linear relationship (R^2 = 0.87) between eLAI and ePAI-eWAI using radiative transfer simulations. Another possible approach is to directly identify woody points in the leaf-on point cloud by using the leaf-off point cloud, since, in theory, the location of these points does not change. However, due to misalignment of these two datasets and wind conditions, the woody points cannot be perfectly matched. In this study we propose a voxel matching approach for the two datasets, leaf-on and leaf-off, to directly identify leaf and woody points. To eliminate confounding clumping effects, we focus on effective parameters (eLAI, ePAI, eWAI) for a direct comparison between airborne LiDAR and terrestrial LiDAR.

Various airborne LiDAR metrics have been used to estimate eLAI (Jensen et al., 2008; Pearse et al., 2017). Using LiDAR metrics to estimate eLAI requires a statistical model to join the metrics with the field measurements of eLAI. Here, we evaluate airborne LiDAR metrics for the estimation of eLAI with a statistical model, using terrestrial LiDAR data as field measurements. This results in a good classification between leaf and woody materials (Li et al., 2018; Ma et al., 2016a).

Our research makes use of airborne LiDAR data acquired in leaf-on and leaf-off conditions for retrieving eLAI. It is worth noting that since leaf-off data are required for calculating eLAI, our study focuses on deciduous forests. We also validate our results using simulated airborne LiDAR point cloud of 3D forest generated by Arbaro (Weber and Penn, 1995) and HELIOS software (Bechtold and Höfle, 2016). We are thus able to evaluate and compare our methods with ground truth eLAI. The aims of our study are to (1) compare the voxel matching method with the subtraction method for estimating effective leaf area index, (2) evaluate the influence of the voxel size used in the voxel matching method when trying to separate woody and leaf points, and (3) assess various leaf-on LiDAR metrics for the estimation of eLAI.

2. Study area and data collection

2.1. Study area

The study area is located in Bavarian Forest National Park (BFNP) in southeastern Germany (Fig. 1). It covers an area of 24,250 ha in size. Being a mountainous area, the elevation ranges from 600 to 1453 m. The major tree species are Norway spruce (*Picea abies*) (67%) and European beech (*Fagus sylvatica*) (24.5%), with some white fir (*Abies alba*) (2.6%), sycamore maples (*Acer psudoplatanus*) (1.2%) and mountain ash (*Sorbus aucuparia*) (3.1%) (Heurich et al., 2010). Data were collected for 36 circular European beech plots of 50 m radius at various elevations. These plots cover young, medium and mature stands and a wide range of stand structures (Liu et al., 2019). The number of trees per plot ranges from 14 to 110 and the ePAI ranges from 0.88 to 4.44.

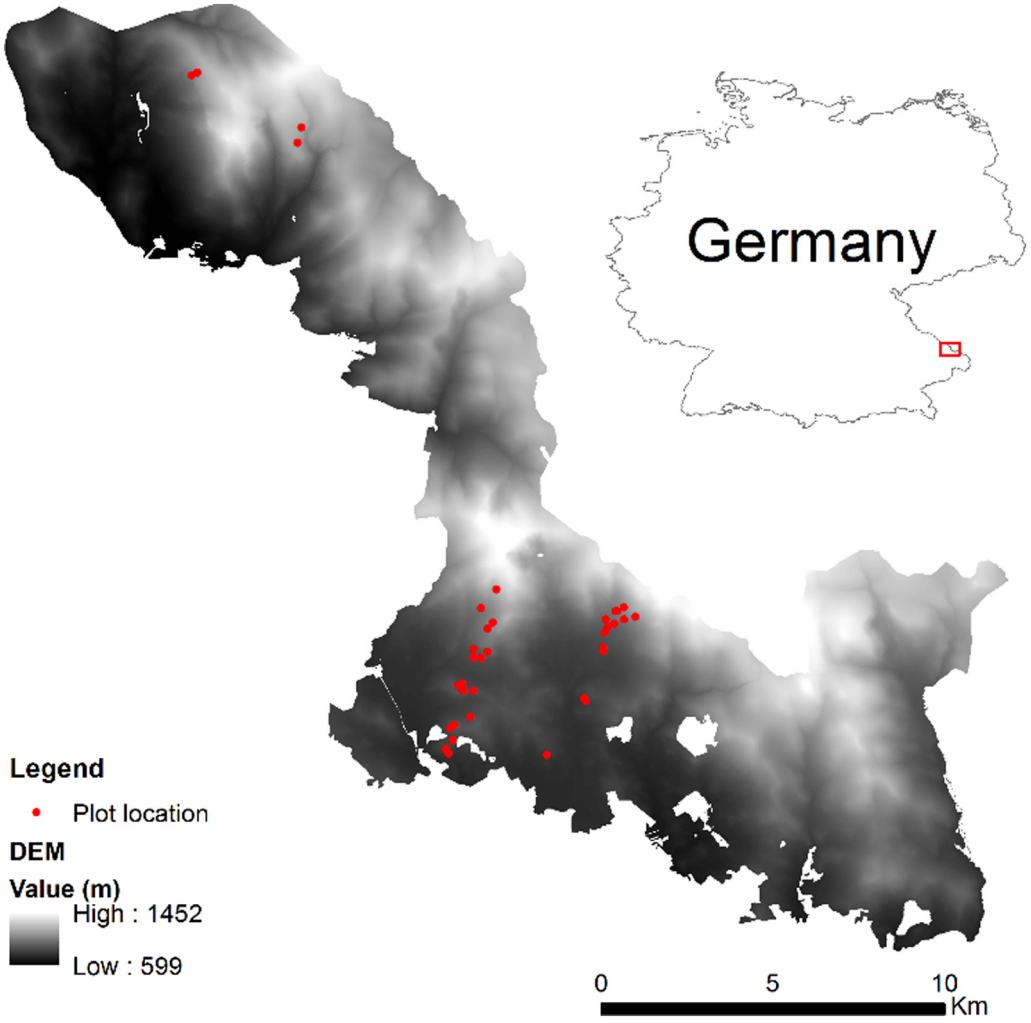

Fig. 1. The distribution of 36 sample plots in the Bavarian Forest National Park.

2.2. Terrestrial LiDAR data collection

Ground data were collected in leaf-on conditions in July 2017, with a Riegl VZ-400, which employs a short-wave infrared (1550 nm) laser. The system has a reported range accuracy of 5 mm, a beam divergence of 0.3 mrad and a maximum range of 600 m. An angular resolution of 0.04° was used with a long-range mode. A center and three triangular scan positions per plot were used to reduce occlusion and increase point density. To register these different scans, 12 cylindrical reflectance targets were placed as control points. Within each plot, a subset of the point cloud with a radius of 50 m was delineated.

2.3. Airborne LiDAR data collection

An airborne LiDAR flight campaign was carried out under both leaf-off and leaf-on conditions, in March and August 2016, respectively. The sensor used was a Riegl LMS-Q 680i, employing a laser with a wavelength of 1550 nm, and a beam divergence of 0.5 mrad. The flying altitude was approximately 300 m above ground, and the data had an average point density of 70 points per m^2.

2.4. LiDAR data simulation

In order to have a 'true' estimate of eLAI to compare our proposed method to, we created a 3D virtual forest of trees with varying leaf density using Arbaro software (Weber and Penn, 1995) (Fig. 2). To model the scene of a leaf-on plot, a random number of trees with random density of leaves was selected within a radius of 50 m (Fig. 3). The size of different trees was multiplied by a random number between 0.5 and 1.5. Corresponding leaf-off plots with the same number and with the trees in the same location were generated by only keeping the woody skeletons. The true leaf area index was obtained based on the area of all leaves in each plot. The point cloud data of the plots were simulated using the laser scanning simulation framework HELIOS. The configuration of the airborne LiDAR was set to match our real data (Section 2.2).

3. Methods

Two methods based on gap fraction theory, namely voxel matching and leaf-on *versus* leaf-off subtraction, were assessed using both field airborne LiDAR data and simulated airborne LiDAR data. An empirical model using various leaf-on field airborne LiDAR metrics was also evaluated. The results were compared with terrestrial LiDAR derived eLAI. The workflow is shown in Fig. 4.

3.1. Estimation of gap fraction

To calculate the gap fraction for both the terrestrial and airborne LiDAR data, the point clouds needed to be classified into ground and non-ground returns. The Lasground module in Lastools (Lastools, rapidlasso GmbH, Germany, 2017) was used for the classification. The

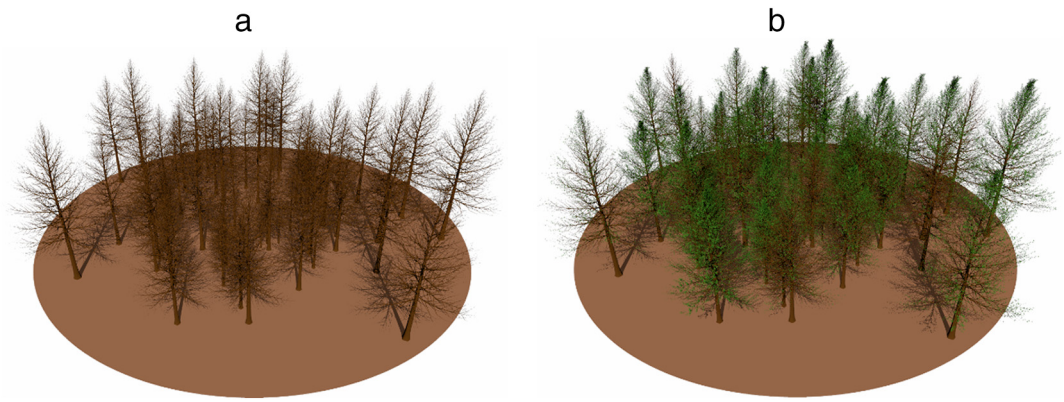

Fig. 2. A complete scene of a forest plot. (a) leaf-off. (b) leaf-on.

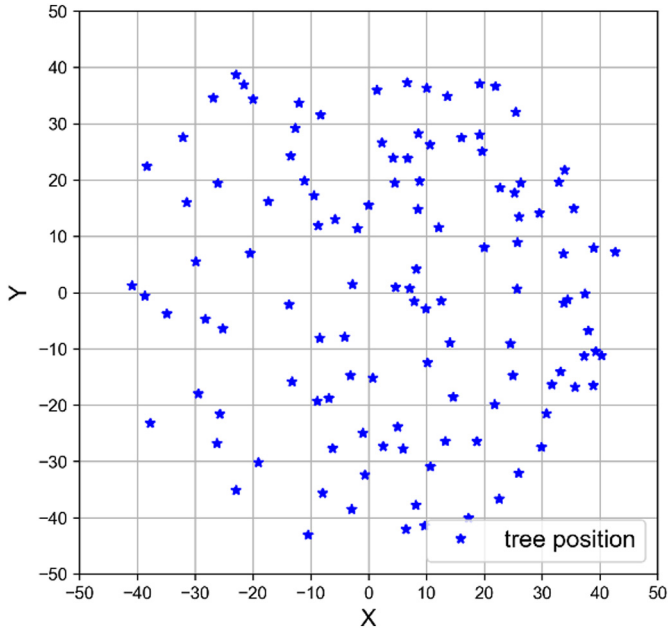

Fig. 3. Random locations of individual trees generated within a plot for data simulation.

height of above-ground points was then calculated as the difference between the return and ground elevation. A "weight all return" method (Armston et al., 2013; Calders et al., 2018), which considers all returns in each pulse, was used (Eq. (1)).

$$P(\theta) = 1 - \frac{\sum 1/NR}{N_{total}} \quad (1)$$

where $P(\theta)$ is the gap fraction at the viewing zenith angle θ, NR is the number of returns detected for each pulse from the canopy, and N_{total} is the total number of outgoing laser pulses. $1/NR$ is a weighted sum of all returns from the canopy. A height threshold of 1.3 m was used to separate canopy and non-canopy returns. This method is hardly sensitive to changing acquisition height and produces near unbiased estimates of gap fraction (Armston et al., 2013).

3.2. ePAI calculation

We calculated eLAI based on the identified leaf points, using well established gap fraction theory (Korhonen et al., 2011; Moorthy et al., 2008). To obtain ePAI from the point cloud, the gap fraction needs to be converted using gap fraction theory based on the Beer-Lambert law (Calders et al., 2018; Nilson, 1971; Solberg et al., 2009; Vincent et al., 2017):

$$ePAI = -\ln(P(\theta)) \cdot \frac{\cos\theta}{G(\theta)} \quad (2)$$

where $G(\theta)$ is the mean projection of a unit leaf area on a plane perpendicular to the direction of the laser beam (Hosoi and Omasa, 2006). The ePAI does not account for foliage clumping index, which quantifies the effect of non-random spatial distribution of foliage (Chen, 1996).

The zenith angle of laser pulses was known for both airborne LiDAR and terrestrial LiDAR. The $G(\theta)$ is approximated based on an ellipsoidal function of the zenith angle and the leaf angle distribution (Campbell, 1986, 1990; Li et al., 2017).

$$G(\theta) = \frac{(\chi^2 + (\tan\theta)^2)^{0.5}\cos\theta}{\chi + 1.774(\chi + 1.182)^{-0.733}} \quad (3)$$

where χ is a shape parameter for the leaf angle distribution, which stands for the ratio of vertical to horizontal projections of canopy elements. A χ value of 2 (close to planofile) (Pisek et al., 2013) was used for the estimation of ePAI, eLAI and eWAI for comparison.

3.3. Retrieval of eLAI and eWAI from terrestrial LiDAR

Previous studies have demonstrated the feasibility and reliability of classifying woody and leaf points using terrestrial LiDAR data (Ma et al., 2016b; Zheng et al., 2016; Zhu et al., 2018). In this study, the method by (Zhu et al., 2018) was adopted to separate leaf and woody components. Both geometric and radiometric features were calculated from terrestrial LiDAR data.

The radiometric features are mainly composed of intensity features. The intensity of terrestrial LiDAR data was calibrated using a white, flat target placed at the same distance from the sensor in each plot (Pfennigbauer and Ullrich, 2010), thus removing the range-dependent effect. Geometric features, consisting of height related features, inclination angle and local dimensionality features, represent the distribution of local points (Table 1). Eigenvalues were used to calculate the local dimensionality properties that describe how the point cloud appears at a given location. In order to obtain the eigenvalues, a local covariance matrix of each point was calculated based on the neighboring points within a radius of a given point. The eigenvalues were sorted in a descending order ($\lambda1 > \lambda2 > \lambda3$). The feature values for these three categories can be expressed as $\lambda1 \gg \lambda2 \approx \lambda3$ for a linear feature, $\lambda1 \approx \lambda2 \gg \lambda3$ for a two-dimensional, flat feature and $\lambda1 \approx \lambda2 \approx \lambda3$ for a 3D random feature (Zheng et al., 2016). Based on the eigenvalues, the local dimensionality features were calculated as follows:

$$\alpha_{1D} = (\sqrt{\lambda_1} - \sqrt{\lambda_2})/\sqrt{\lambda_1},\ \alpha_{2D} = (\sqrt{\lambda_2} - \sqrt{\lambda_3})/\sqrt{\lambda_1},\ \alpha_{3D} = \sqrt{\lambda_3}/\sqrt{\lambda_1} \quad (4)$$

where α_{1D}, α_{2D} and α_{3D} represent the likelihood that the shape of local points around the given point is linear, planar and random,

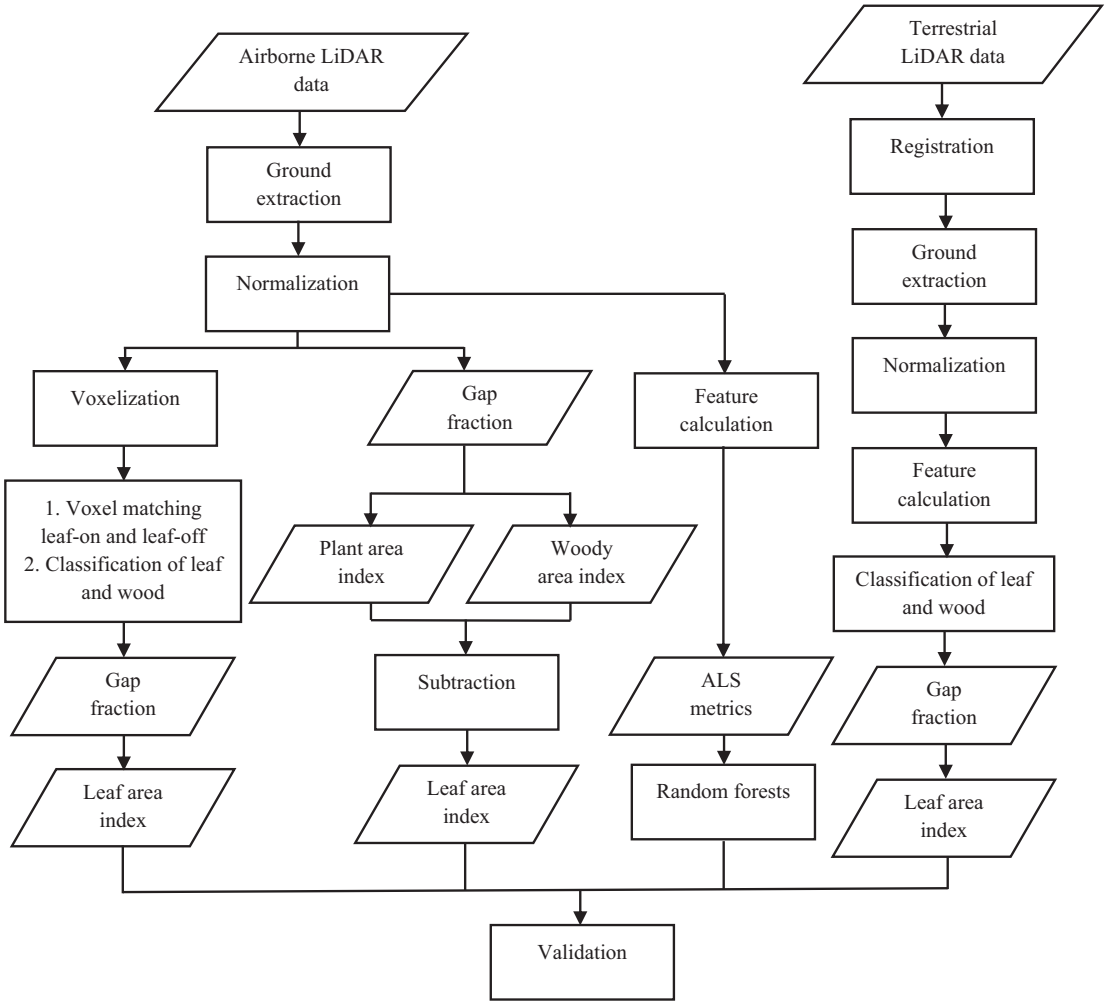

Fig. 4. Work flow diagram for eLAI estimation.

respectively. The zenith angle and mean zenith angle of local points were also included in the classification, since leaves had different zenith angles from branches. eLAI and eWAI were calculated following the classification using the gap fraction method.

A random forest classification was applied, as this algorithm is not sensitive to highly correlated features and is both fast and insensitive to overfitting (Belgiu and Drăguţ, 2016). To train the random forest classifier, training samples were manually selected from the point cloud and were identified as either leaf or woody points (Zhu et al., 2018). The terrestrial LiDAR derived features (Table 1) of the training samples were used as input in the random forest classifier. The number of trees was set to 100 (Guan et al., 2013). Subsequently, the model was applied to the whole point cloud.

3.4. Retrieval of eLAI and eWAI from leaf-on and leaf-off airborne LiDAR

Two methods were tested and compared in this study in order to calculate eLAI from airborne LiDAR data in leaf-on and leaf-off conditions: (1) a direct subtraction of eWAI from leaf-off data, (2) a voxel matching approach to separate woody points from leaf points.

3.4.1. ePAI – eWAI (method 1(M1))

The ePAI and eWAI were calculated for leaf-on and leaf-off data, respectively, based on Eqs. (1), (2) and (3). Subsequently, eLAI was obtained by subtracting eWAI from ePAI.

Table 1
List of the features extracted for classification from terrestrial LiDAR data.

Type	Feature	Definition	Reference
Radiometric features	I	Backscatter intensity	Pfennigbauer and Ullrich (2010)
	I_{mean}	Mean intensity of the local points	Koenig et al. (2015)
	I_{cov}	Intensity coefficient of variation of the local points	Koenig et al. (2015)
Geometric features	α_{1D}	The likelihood that the shape of the local points is linear (1D)	Demantke et al. (2011)
	α_{2D}	The likelihood that the shape of the local points is planar (2D)	Demantke et al. (2011)
	α_{3D}	The likelihood that the shape of the local points is random (3D)	Demantke et al. (2011)
	StdZ	Standard deviation of the height values	Koenig et al. (2015)
	Zdiff	Range of maximum and minimum height value	Koenig et al. (2015)
	ZA	Zenith angle of local points	
	ZA_{mean}	Mean zenith angle of local points	

3.4.2. Voxel matching (method 2(M2))

A voxel is defined as a cubic element in a 3D array. All LiDAR points from leaf-on and leaf-off data were converted into voxel coordinates, since exact matching of the woody points in these two datasets could not be achieved due to wind effects and system accuracy. The voxelization allows voxels that represent woody points to intersect. The voxelization was executed based on (Hosoi and Omasa, 2006):

$$i = Int\left(\frac{X - X_{min}}{\Delta i}\right) \tag{5}$$

$$j = Int\left(\frac{Y - Y_{min}}{\Delta j}\right) \tag{6}$$

$$k = Int\left(\frac{Z - Z_{min}}{\Delta k}\right) \tag{7}$$

where i, j, and k are the voxel coordinates in the 3D array, Int means to round off at one decimal place to the nearest integer, X, Y, and Z stand for the original point coordinates of the LiDAR data, X_{min}, Y_{min}, and Z_{min} are the minimum values of X, Y, and Z, respectively, and Δi, Δj, and Δk denote the voxel size. In this study, voxel sizes from 0.05 m to 0.5 m, applying steps of 0.05 m, were assessed for the classification. A voxel size of 0.1 m represents a cube size of 0.1 × 0.1 × 0.1 m. The voxels containing LiDAR hits corresponding with leaf-on as well as leaf-off datasets were identified as woody points, while the others were recognized as leaf points. Then leaf canopy cover (1-gap fraction) was calculated based on leaf points, while the woody canopy cover was calculated based on the matched woody points. Finally, eLAI and eWAI were calculated using gap fraction theory (Eq. (2)).

3.5. Evaluation of eWAI using voxel matching

We evaluated voxel matching by quantifying the matched and unmatched eWAI which constitute the eWAI derived from airborne leaf-off LiDAR data. The matched eWAI observed by leaf-on LiDAR data was derived from the woody gap fraction based on the intersecting woody points in the leaf-on data using the voxel matching method. The unmatched eWAI was obtained by subtracting the matched eWAI from the total eWAI obtained from the leaf-off data. A Pearson's correlation test was used to evaluate the relationship between the proportion of unmatched eWAI relative to the total eWAI and ePAI.

3.6. Retrieval of eLAI based on an empirical method using leaf-on airborne LiDAR only

Based on literature review, a list of common leaf-on metrics (Table 2) for the estimation of eLAI was assembled, including height metrics (Pearse et al., 2017; Shi et al., 2018), ratio metrics (Næsset and Bjerknes, 2001) and radiometric metrics (Luo et al., 2018; Vauhkonen et al., 2010). These metrics were derived using LiDAR processing software Fusion (McGaughey, 2009). In addition, 4 LiDAR penetration metrics commonly used for estimating canopy cover were added (Armston et al., 2013; Korhonen et al., 2011; Lovell et al., 2011; Solberg et al., 2009) (Table 2).

A random forest regression was used to estimate eLAI. Random forest regression offers sophisticated measures of variable importance beyond rank and selection frequency (Pearse et al., 2017). It is a non-parametric statistical method that improves the estimation accuracy and reduces overfitting (Gleason and Im, 2012). Random forest regression has been successfully applied to estimating eLAI based on LiDAR metrics (Luo et al., 2018; Pearse et al., 2017). Its strength is discovering nonlinear relationships in high dimensional data where independent variables show high levels of correlation (Criminisi et al., 2012). To select important features and to avoid overfitting, 'variable importance' was adopted, following training of the random forest algorithm. The most important predictors with an importance score larger than 0.01 were used to re-fit and construct the random forest model (Cutler et al. 2012). The number of regression trees in this study was set at 1500 instead of the default quantity of 500 for more accurate results. The random forest model was subsequently applied to predict the eLAI with the test dataset.

For an unbiased assessment of a model, a held-out test to create a validation dataset independent of the calibration dataset is recommended. However, insufficient field plots were available to provide an independent validation dataset. Therefore, a leave-one-out cross-validation method, as used to validate forest attributes with airborne LiDAR data, was applied to evaluate the random forest model (Bouvier et al., 2015; Pearse et al., 2017; Picard and Cook 1984; Véga et al. 2016).

3.7. Statistical analysis

The results were evaluated based on the coefficient of determination (R^2), the root mean square error (RMSE), the relative RMSE (RRMSE) and the bias. A significance test was also carried out.

$$R^2 = 1 - \frac{\sum (y_i - y_i')^2}{\sum (y_i - \bar{y})^2} \tag{8}$$

$$\text{RMSE} = \sqrt{\frac{\sum (y_i - y_i')^2}{n}} \tag{9}$$

$$\text{Bias} = \frac{\sum (y_i - y_i')}{n} \tag{10}$$

$$\text{RRMSE} = \frac{RMSE}{\bar{y}} \tag{11}$$

where y_i and y_i' are the measured and estimated values for sample i, respectively, and $\overline{y_i}$ and n denote the mean and the number of samples, respectively.

4. Results

4.1. Estimation of effective leaf area index when using real field data

Fig. 5a shows that PAI values derived from real leaf-on data were significantly correlated with observed values derived from terrestrial LiDAR with a low RMSE and bias ($R^2 = 0.75$, $p < .05$). Based on the subtraction method, eLAI was considerably underestimated using the real data (Fig. 5b).

The effect of voxel size on the estimation of eLAI using the voxel matching method is summarized in Fig. 6. A voxel size of 0.1 m achieved the highest value of R^2 for the estimation of eLAI, while both the RMSE value and the absolute value of bias were minimized at this voxel size. The voxel size of 0.1 m was consequently chosen for further analysis.

Subsequently eWAI and eLAI estimated using a voxel size of 0.10 m were validated against those derived from terrestrial LiDAR data. Both estimates showed significant correlation and low RMSE and bias values. Compared to the estimation of eLAI based on subtraction, the errors, especially the underestimation of eLAI, decreased significantly (Fig. 7).

4.2. Comparison between the subtraction and voxel matching method

The comparison of eLAI estimation between subtraction and voxel matching can be seen in Fig. 8. A strong correlation emerged between these two methods for eLAI estimation. However, the estimates of eLAI based on the subtraction method were on average 0.96 lower than those based on the voxel matching method.

Table 2
List of leaf-on airborne LiDAR metrics for the estimation of eLAI.

Metrics	Definition
Penetration ratio metrics	
FCI (First echo Cover Index)	$\frac{\sum Single_{canopy} + First_{canopy}}{\sum Single_{all} + First_{all}}$
DI (weighted Discrete Index)	$1 - \frac{\sum 1/NR}{N_{total}}$ (NR is the number of returns, and N_{total} is the total number of outgoing laser pulses)
LCI (Last echo Cover Index)	$\frac{\sum Single_{canopy} + Last_{canopy}}{\sum Single_{all} + Last_{all}}$
SCI (Solberg Cover Index)	$1 - \frac{\sum Single_{ground} + 0.5(\sum First_{ground} + \sum Last_{ground})}{\sum Single_{all} + 0.5(\sum First_{all} + \sum Last_{all})}$
Total return count	Total number of returns
Return 1–9 count	Count of returns (1–9)
Height metrics	
Elev minimum	Minimum
Elev maximum	Maximum
Elev mean	Mean
Elev mode	Mode elevation
Elev stddev	Standard deviation
Elev variance	Variance
Elev CV	Coefficient of variation
Elev IQ	Interquartile distance
Elev skewness	Skewness
Elev kurtosis	Kurtosis
Elev AAD	Average Absolute Deviation
Elev MAD median	Median of the absolute deviations from the overall median
Elev MAD mode	Median of the absolute deviations from the overall mode
Elev L 1–4	L-moments 1–4
Elev L CV	L-moment Coefficient of variation
Elev L skewness	L-moment skewness
Elev L kurtosis	L-moment kurtosis
Elev P01, P05, P10, P20, P25, P30, P40, P50, P60, P70, P75, P80, P90, P95, P99	Percentile values (1st, 5th, 10th, 20th, 25th, 30th, 40th, 50th, 60th, 70th, 75th, 80th, 90th, 95th, 99th percentiles)
Canopy relief ratio	Canopy relief ratio ((mean - min) / (max – min))
Elev SQRT mean SQ	Generalized means for the 2nd and 3rd power (Elev quadratic mean)
Elev CURT mean CUBE	Generalized means for the 2nd and 3rd power (Elev cubic mean)
Intensity metrics	
Int minimum	Minimum
Int Maximum	Maximum
Int mean	Mean
Int mode	Mode elevation
Int stddev	Standard deviation
Int variance	Variance
Int CV	Coefficient of variation
Int IQ	Interquartile distance
Int skewness	Skewness
Int kurtosis	Kurtosis
Int AAD	Average Absolute Deviation
Int L 1–4	L-moments 1–4
Int L CV	L-moment Coefficient of variation
Int L skewness	L-moment skewness
Int L kurtosis	L-moment kurtosis
Int P01, P05, P10, P20, P25, P30, P40, P50, P60, P70, P75, P80, P90, P95, P99	Percentile values (1st, 5th, 10th, 20th, 25th, 30th, 40th, 50th, 60th, 70th, 75th, 80th, 90th, 95th, 99th percentiles)
Percentage first returns above mean	Percentage of first returns above the mean height
Percentage first returns above mode	Percentage of first returns above the mode height
Percentage all returns above mean	Percentage of all returns above the mean height
Percentage all returns above mode	Percentage of all returns above the mode height
(All returns above mean)/(Total first returns) *100	Number of returns above the mean height/total first returns ∗ 100
(All returns above mode)/(Total first returns) *100	Number of returns above the mode height/total first returns ∗ 100
First returns above mean	Number of first returns above the mean height
First returns above mode	Number of first returns above the mode height
All returns above mean∗	Number of all returns above the mean height
All returns above mode	Number of all returns above the mode height

4.3. Estimation of effective leaf area index based on simulation

The simulation of point clouds for different LAI values is shown in Fig. 9. Both leaf-off and leaf-on plots were simulated so the methods for extracting LAI and WAI could be tested and compared.

We conducted an accuracy assessment for the classification between leaf and woody points using the voxel matching method (voxel size: 0.1 m) on the simulation data. Each point in the simulated data was labeled as leaf or woody for validation. Fig. 10 presents the overall classification accuracy, as well as precision and recall for the leaf points. Classification using the voxel matching method achieved an average overall accuracy of 0.83. The average recall of leaf points was 0.99, indicating that the omission error of leaf points was very low. The precision of leaf points (average 0.82), on the other hand, showed that a proportion of the woody points was misclassified as leaf points, which could be caused by mismatching between the small voxels. The lowest

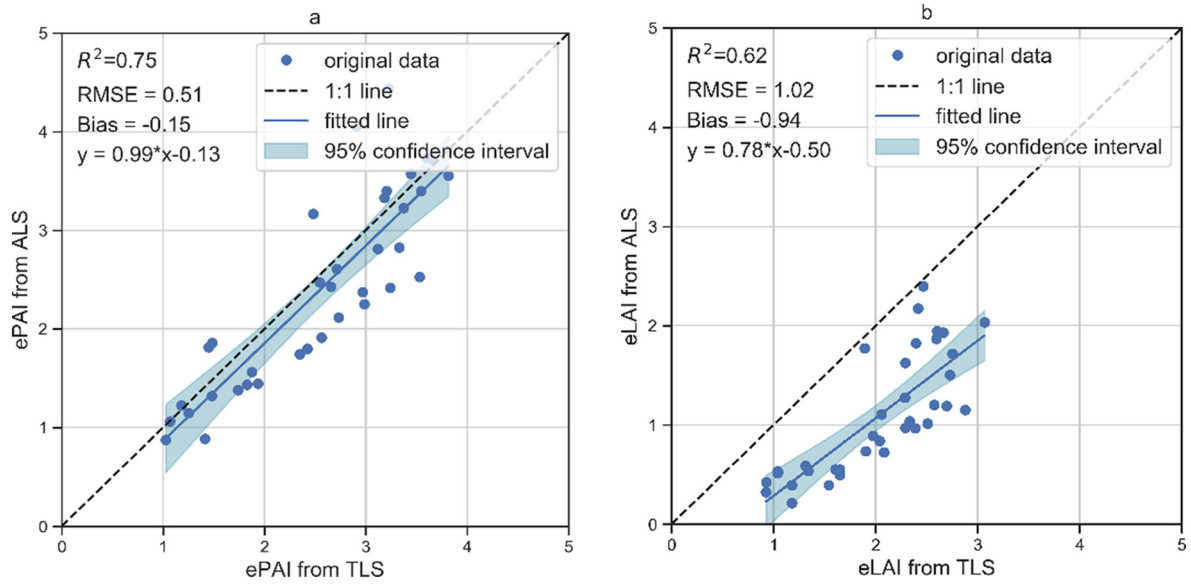

Fig. 5. Validation of ePAI and eLAI (using subtraction method) using only leaf-on data validated by terrestrial LiDAR. (a) Validation of ePAI, (b) Validation of eLAI using subtraction method.

accuracy observed for a plot, combined with a precision of 0.60, was due to the low LAI value of 0.01. Few points were sampled in this plot.

The results for the estimation of eLAI in 30 plots using the two different methods tested in this study are presented in Fig. 11. The bias of −0.57 (Fig. 11a) shows that the eLAI calculated by subtracting leaf-off eWAI from leaf-on ePAI significantly underestimated the observed eLAI, although the correlation with the observed eLAI was strong (R^2 = 0.93). The voxel matching method generated a much lower bias as well as a higher value of R^2. It is noteworthy that for plots with higher eLAI values, the underestimation of the observed eLAI based on the subtraction method was higher. There was clearly a significant relationship between the underestimation of eLAI using the subtracting method and the eLAI. This indicates that plot density had a strong impact on eLAI estimation using the subtraction method.

4.4. Evaluation of eWAI using voxel matching

The estimations of matched eWAI and unmatched eWAI for each plot are shown in Fig. 12. The Pearson's test showed that the proportion of unmatched eWAI to total eWAI was significantly correlated with eLAI estimated from airborne LiDAR with a *p*-value < .01 (Fig. 13). Visually, it can also be seen that many trunk voxels (in black) from the leaf-off data were not matched in the leaf-on data (Fig. 14).

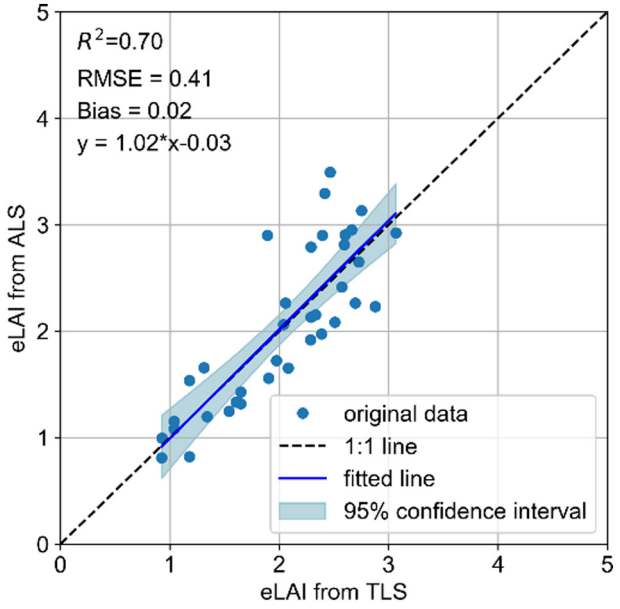

Fig. 7. Validation of eLAI estimation based on voxel matching using real data.

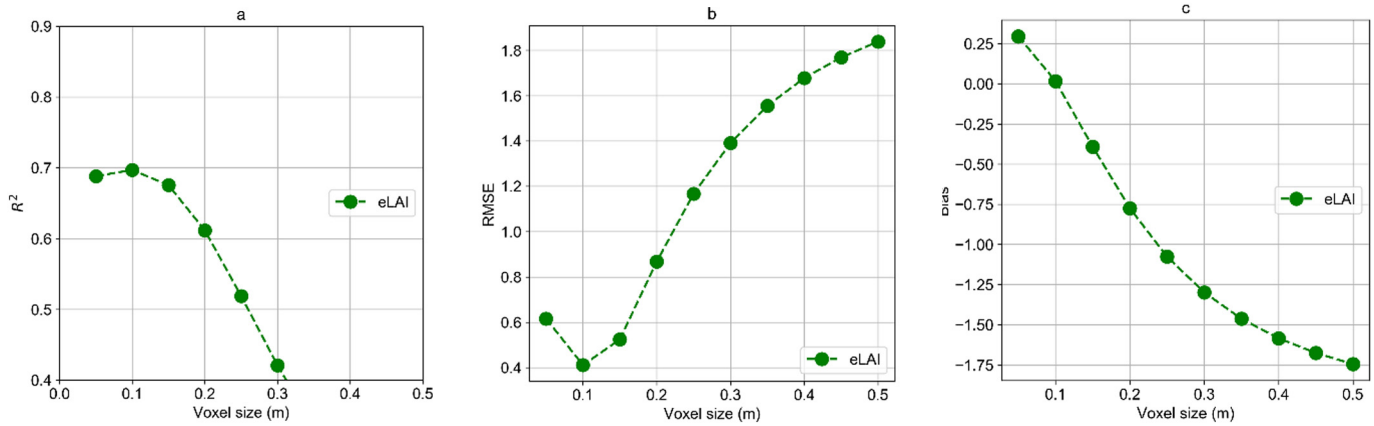

Fig. 6. The influence of voxel size on the estimation accuracy of eLAI using voxel matching method. (a) R^2 value, (b) RMSE value, (c) bias value.

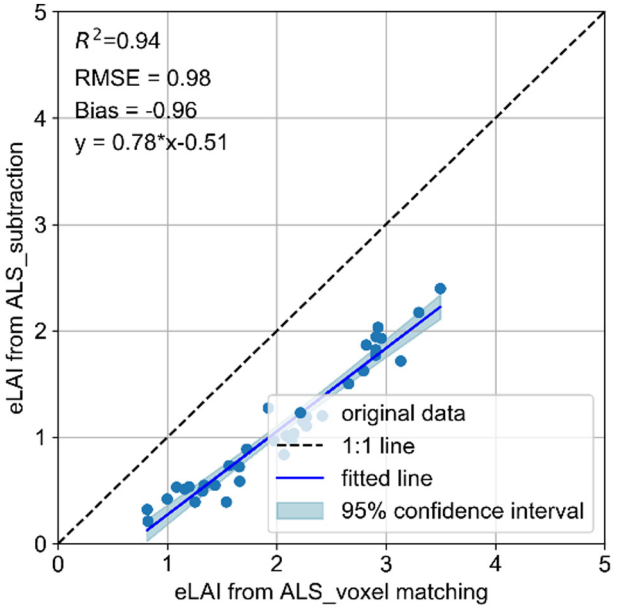

Fig. 8. Comparison of eLAI estimation between subtraction and voxel matching.

4.5. Linking leaf-on airborne LiDAR metrics with effective leaf area index

Importance scores derived from random forest regression are presented in Fig. 15, with variables scoring above 0.01 depicted. The top five most important LiDAR metrics were FCI, SCI, DI, LCI and Elev P01, which are height and penetration ratio metrics.

The validation for eLAI was established based on the most important leaf-on LiDAR metrics with an importance score larger than 0.01 (Fig. 15) using random forest regression. The results show that eLAI could be estimated with an accuracy of R^2 = 0.73 and RMSE = 0.27 (Fig. 16).

5. Discussion

We found significant correlation, with an R^2 value of 0.70, between airborne LiDAR derived effective leaf area index (eLAI) and terrestrial LiDAR derived eLAI using the voxel matching method. Voxel matching produced a much lower RMSE of 0.41 (RRMSE: 20.1%) than the subtraction method (RMSE: 1.02, RRMSE: 50.1%). The subtraction method significantly underestimated eLAI by 0.94 on average, compared to an underestimation of 0.02 using the voxel matching method. The same outcome was largely observed when using the simulated dataset. The results support the use of the voxel matching method for the estimation of eLAI in deciduous forests using leaf-on and leaf-off airborne LiDAR data.

Subtracting the effective woody area index (eWAI) obtained in leaf-off conditions from the effective plant area index (ePAI) in the leaf-on state can cause significant underestimation of eLAI. The underestimation is partially caused by the fact that a large proportion of woody materials present in the leaf-off scan were occluded by leaves in the leaf-on scan. As the canopy becomes denser, the underestimation increases, because more woody materials are occluded by the additional leaves. Another possible reason is that LiDAR signal might be saturated in dense canopies. In dense forests, canopy cover of only woody components using leaf-off data can be very high, as most of the returns are intercepted by trunks and branches. When leaves are present, saturation occurs where canopy cover does not increase with plant area anymore. Therefore, subtracting eWAI in leaf-off conditions from ePAI in the leaf-on state could cause erroneous calculation of eLAI.

Comparison between the two methods, subtraction and voxel matching, further validated our results (Fig. 8). The strong correlation of results when using these two completely different methods indicates the robustness of the voxel matching method. The underestimation of eLAI using the subtraction method appears to be amplified for higher LAI values. We demonstrated the influence of LAI on the underestimation of eLAI using the subtraction method (see Fig. 11). Our findings, therefore, suggest that voxel matching should be used to estimate eLAI in deciduous forests using leaf-on and leaf-off data.

An appropriate voxel size needed to be determined for accurate eLAI

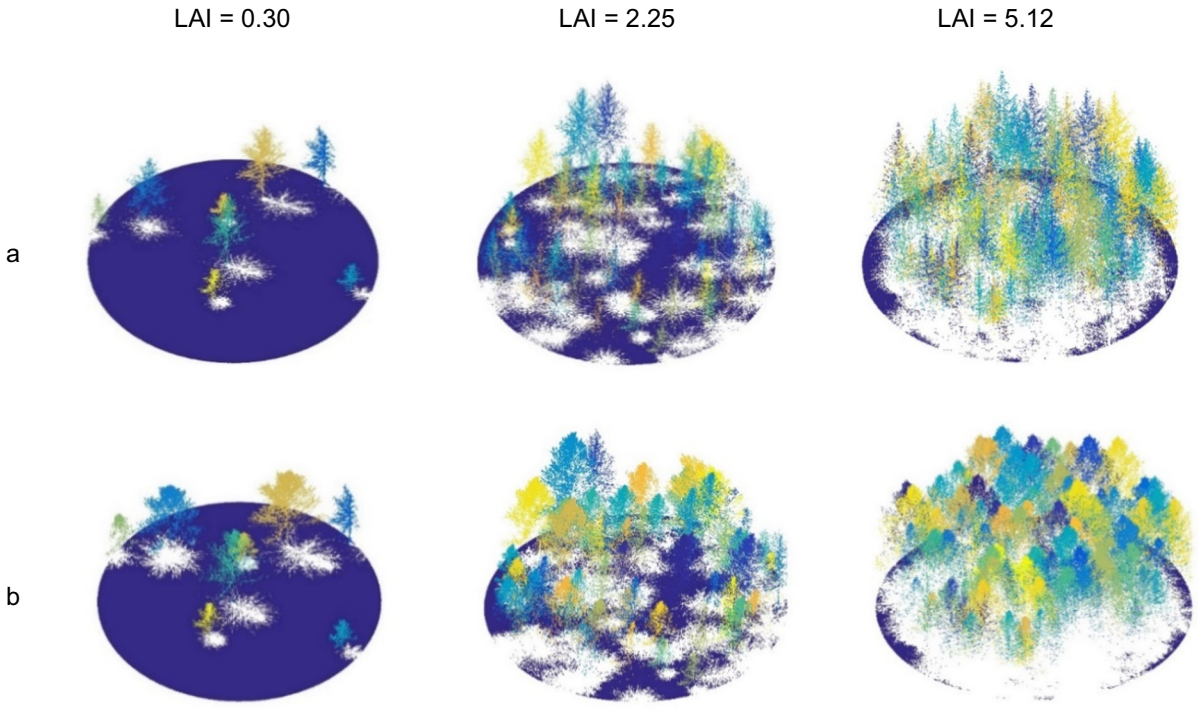

Fig. 9. Simulations of airborne LiDAR point cloud using Helios software. (a) leaf-off. (b) leaf-on.

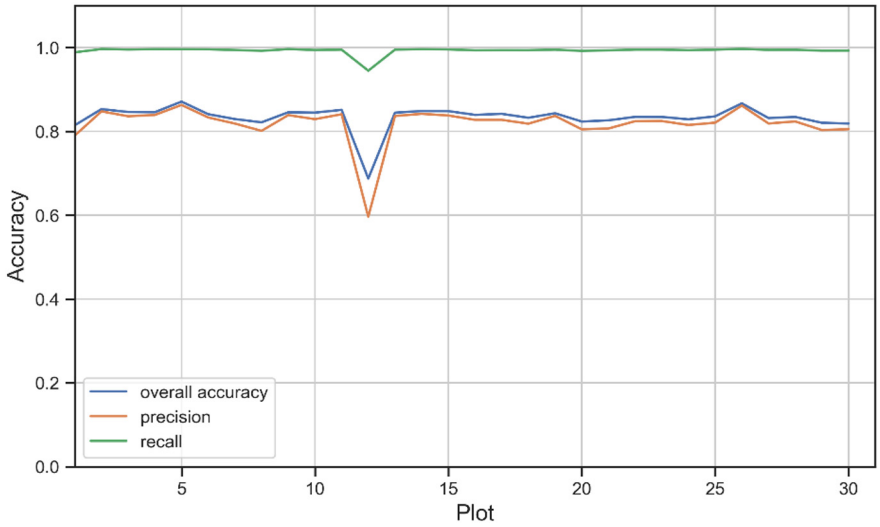

Fig. 10. Assessment of classification accuracy of leaf points (blue line: overall accuracy, red line: precision of leaf points, green line: recall of leaf points). (For interpretation of the references to colour in this figure legend, the reader is referred to the web version of this article.)

estimation. We evaluated the effect of voxel size ranging from 0.05 m to 0.5 m, using steps of 0.05 m, bearing the distance of two consecutive points (about 0.15 m) in mind. We demonstrate that, as the voxel size increased, R^2 of the eLAI estimation decreased. A larger voxel would result in more voxels matching between leaf-on and leaf-off scans. As a consequence, a larger proportion of leaf hits would be identified as woody hits leading to an underestimation of eLAI. On the other hand, with a small voxel, some woody points might not be identified due to misalignment of the two scans, causing an overestimation of eLAI. Our results show that RMSE values of eLAI appear to be the lowest at a voxel size of 0.1 m. This voxel size is large enough for most woody hits to match up despite misalignment due to precision and wind, and small enough to exclude mixed voxels and leaf hits in the voxel matching.

The evaluation of eWAI in §4.4 shows that a large proportion of woody points were not matched between leaf-off and leaf-on scans. This is mainly attributed to the occlusion of woody components by leaves, so that these points were not seen in the leaf-on data. Other possible explanations could be the misalignment which may occur between the leaf-on and leaf-off scans when the spatial accuracy of the LiDAR data is not high enough, or strong wind is present during the flight campaign, forms the main disadvantage of the voxel matching method. Since the leaf-on and leaf-off scans were acquired in the same year, the influence of tree growth is expected to have been negligible. Another important factor that needs to be taken into account is the point density. In theory, to match the woody points in leaf-on and leaf-off scans, the point density of the leaf-off scan should be equal or higher than that of the leaf-on scan, so that most woody points in the leaf-on scan can be identified and deducted in the calculation of eLAI. The impact of point density in leaf-on and leaf-off scans will need to be further evaluated.

The importance score generated by the random forest regression showed that the most important metrics to estimate eLAI are penetration ratio metrics and height metrics (Fig. 15). Ratio metrics such as FCI, SCI, DI and LCI have been frequently used to estimate eLAI (Armston et al., 2013; Hopkinson and Chasmer, 2009; Solberg et al., 2009). In this study, the first three metrics (FCI, SCI and DI) are highly correlated with an average R^2 of 0.99. These ratio metrics all provide a measure of gap fraction through ratios of pulse penetration that can be directly linked to eLAI. Height metrics had a much lower importance score, indicating that penetration metrics are more important than height metrics for the estimation of eLAI. This is in agreement with the

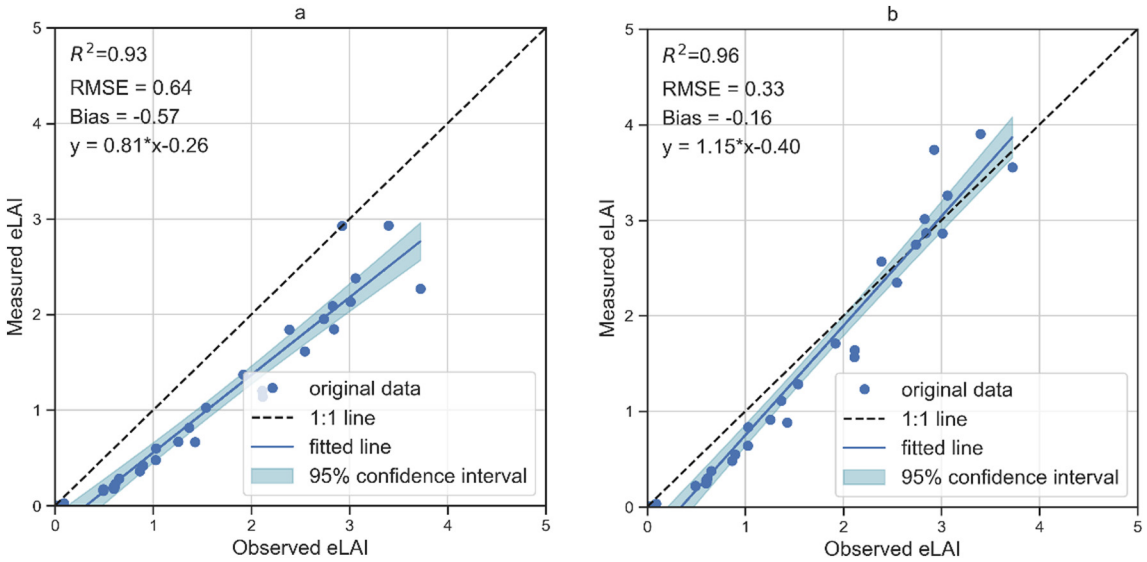

Fig. 11. Validation of the estimation of LAI based on simulated data for 30 simulated plots using different methods: (a) ePAI – eWAI (M1), (b) Voxel matching (M2).

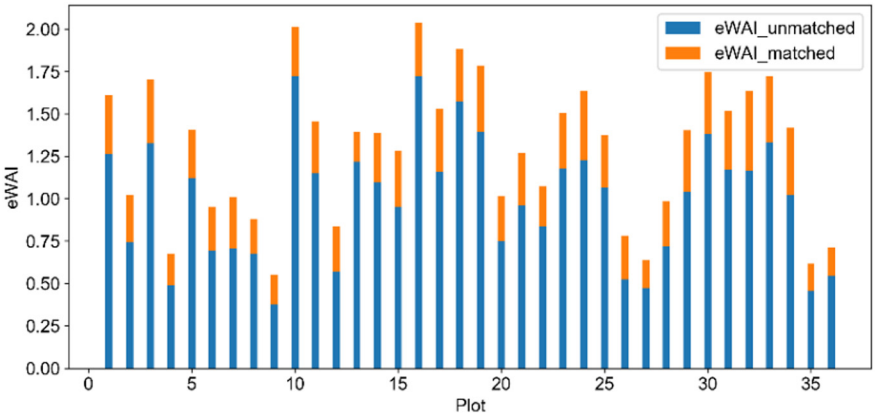

Fig. 12. Matched eWAI and unmatched eWAI in leaf-on data (orange bar: included eWAI, blue bar: occluded eWAI). (For interpretation of the references to colour in this figure legend, the reader is referred to the web version of this article.)

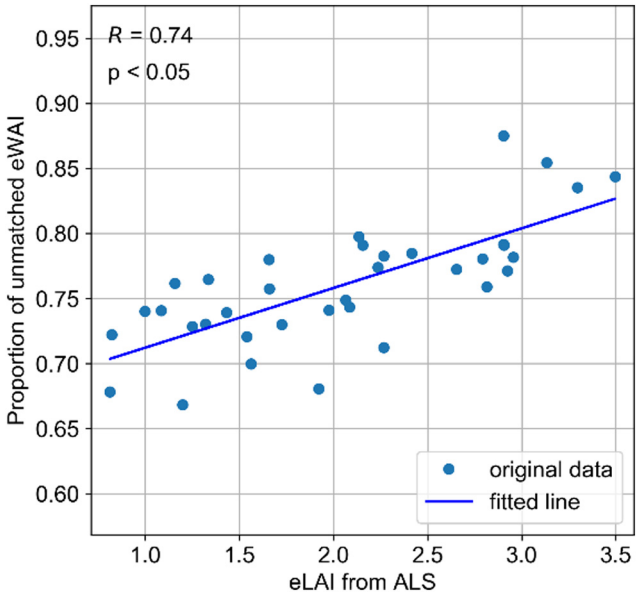

Fig. 13. Pearson's correlation test between ePAI derived from airborne LiDAR and the percentage of unmatched eWAI.

study by (Pearse et al., 2017) who also found that penetration metrics contributed more to eLAI estimation.

With the statistical method, an R^2 of 0.73 and an RMSE of 0.27 (RRMSE: 13.3%) were achieved, in spite of only using a leaf-on scan. It is hard to compare our results with previous studies, as obtaining eLAI through terrestrial LiDAR classification for validation has not previously been attempted (Ma et al., 2016a, 2017). Most frequently, field measurement of LAI has been executed with optical instruments, which do not provide good separation between woody and leaf materials. While a clear comparison of accuracy may not be feasible, previous studies did indicate that statistical models provided higher accuracy than physically based models (Pearse et al., 2017). However, with statistical models being site and flight campaign dependent, accuracy could vary for different sites even within one study (Jensen et al., 2008). This poor transferability between sites and flight campaigns forms the main disadvantage of statistical models (Armston et al., 2013; Pearse et al., 2017). Training and calibration of a new model are needed every time the tree species, the canopy structure, the LiDAR sensor or the flight parameters change. Our voxel matching method yielded an R^2 of 0.70 and an RMSE of 0.41 (RRMSE: 20.1%), which was close in accuracy to that obtained using the statistical model. It is worth mentioning that the training and test datasets were the same (leave-one-out). On the other hand, the 36 plots were all used as test dataset for the voxel matching method. Potentially, the voxel matching method could be directly applied to airborne LiDAR data of another study area. The penetration ratio used in this study to estimate gap fraction (Armston et al., 2013) and the conversion from gap fraction to eLAI have been proved effective in different study areas with different sensors (Armston et al., 2013; Calders et al., 2018; Lovell et al., 2011). However, the matching between leaf-on and leaf-off data requires relatively high

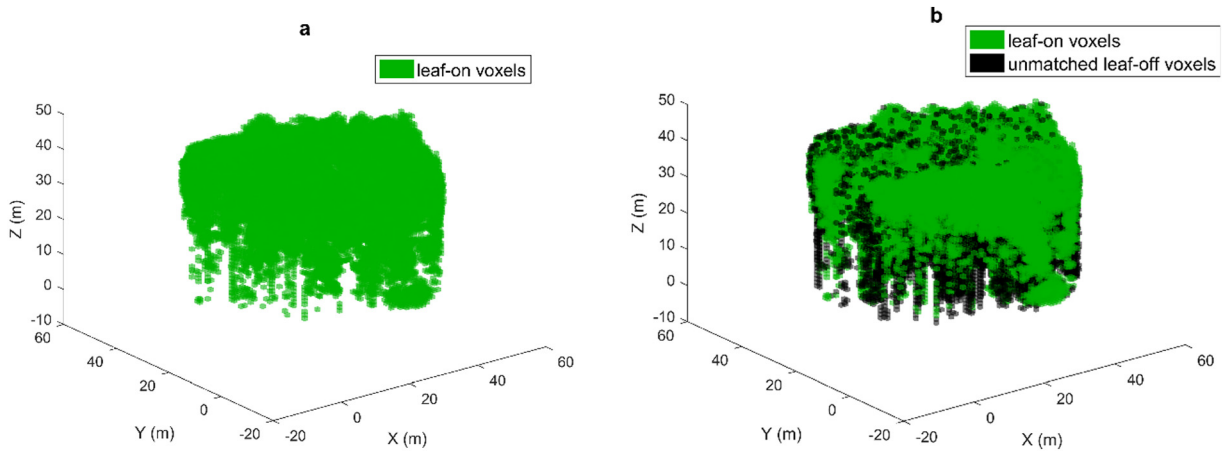

Fig. 14. Voxelization of leaf-on and leaf-off data. (a) leaf-on voxels. (b) leaf-on and unmatched leaf-off voxels (green voxels: leaf-on voxels, black voxels: unmatched voxels). (For interpretation of the references to colour in this figure legend, the reader is referred to the web version of this article.)

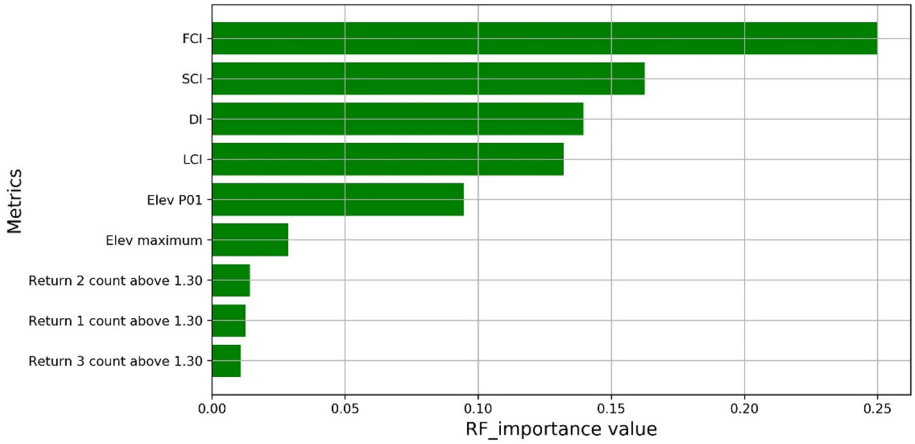

Fig. 15. Importance scores of leaf-on LiDAR metrics to estimate eLAI using Random Forest regression (only variables with an importance score higher than 0.01 are shown).

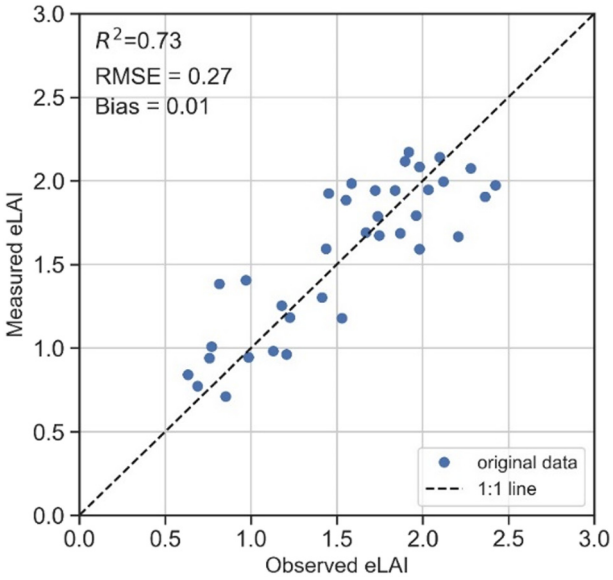

Fig. 16. Validation using terrestrial LiDAR derived eLAI (observed eLAI) for the estimation of eLAI using important leaf-on LiDAR metrics based on random forests regression.

point density. The minimum point density for the voxel matching method to work is yet to be addressed. The relationship between the voxel size and point density needs be modeled using various point densities. So when applying the method to other studies, the voxel size could be predetermined based on the model. Future work will be focused on the dependency of the voxel size on point density.

Although the voxel matching method provided slightly lower accuracy than the statistical method, the voxel matching method is not limited to the estimation of eLAI. It provides a new way to classify leaf and woody materials using airborne LiDAR data. The estimation of other leaf properties such as biochemical parameters that requires the separation of leaf materials from wood materials can benefit from the voxel matching method. It would also open up other ecological applications, especially those to do with radiation transfer, gas exchange and net primary production partitioning of different materials (Vicari et al., 2019).

However, the joint use of leaf-on and leaf-off data does limit the application of the proposed voxel matching approach to deciduous forests. Deciduous forests are of immense importance for biodiversity (Norden et al., 2018), as well as for providing a wide variety of ecosystem services, such as carbon storage, water purification and food provision (Nilsson, 2016). The accurate estimation of eLAI can further improve the evaluation of the relationship between eLAI and biological and physical processes. Though the leaf-on and leaf-off images collected by the Bavarian Forest National Park were not designed to map LAI, but rather for many other applications, such as tree phenology studies, the estimation of forest structural parameters, DEM extraction, understory assessment and tree species classification (Hill and Broughton, 2009; Kim et al., 2009; Næsset, 2005; Parent and Volin, 2014; White et al., 2015), it is of interest to the Park authority that the LiDAR imagery can be used to accurately estimate LAI. The method proposed here can well be applied in future studies using UAV LiDAR, as it is cost efficient and flexible for multi-temporal observation. With the point density being much higher, the method proposed in this study is expected to lead to a higher accuracy.

6. Conclusions

We introduced a new voxel matching method to classify leaf and woody points using leaf-off and leaf-on airborne LiDAR data. Our results demonstrate the applicability of this method in temperate deciduous forests for the estimation of eLAI. Another method based on gap fraction theory, the subtraction method, shows close correlation with the voxel matching method, but significantly underestimates eLAI by subtracting the occluded woody materials in leaf-off data. Empirical approaches benefit from the simplicity of their methods and the fact that only leaf-on data are required. However, they suffer from the necessity of re-calibration every time the tree species, canopy structure and LiDAR sensor change. The voxel matching method offers the potential to estimate eLAI with greater transferability without the need for re-calibration. It is worth noting that the voxel matching method is dependent on the point density. High point density would render the matching between leaf-off and leaf-on scans possible. In particular, the point density of the leaf-off scan should be equal or higher than that of the leaf-on scan. The minimum point density for voxel matching to be applicable needs to be quantified. The present research, especially the classification, is validated primarily with simulated data. Future work would also benefit from the inclusion of 'ground truth' classification data of leaf and woody materials.

CRediT authorship contribution statement

Xi Zhu: Conceptualization, Methodology, Software, Validation, Formal analysis, Writing - original draft. **Jing Liu:** Methodology, Investigation, Writing - review & editing. **Andrew K. Skidmore:** Resources, Writing - review & editing, Supervision, Funding acquisition. **Joe Premier:** Investigation, Writing - review & editing. **Marco**

Heurich: Investigation, Writing - review & editing, Project administration.

Declaration of competing interest

The authors declare that they have no known competing financial interests or personal relationships that could have appeared to influence the work reported in this paper.

Acknowledgements

This research is funded by the Natural Resources Department, ITC, University of Twente. We thank the "Data Pool Forestry" data-sharing initiative of the Bavarian Forest National Park. This project has received funding from the European Research Council (ERC) under the European Union's Horizon 2020 research and innovation programme (grant agreement number 834709).

References

Alonzo, M., Bookhagen, B., McFadden, J.P., Sun, A., Roberts, D.A., 2015. Mapping urban forest leaf area index with airborne lidar using penetration metrics and allometry. Remote Sens. Environ. 162, 141–153.
Armston, J., Disney, M., Lewis, P., Scarth, P., Phinn, S., Lucas, R., Bunting, P., Goodwin, N., 2013. Direct retrieval of canopy gap probability using airborne waveform lidar. Remote Sens. Environ. 134, 24–38.
Asrar, G., Fuchs, M., Kanemasu, E.T., Hatfield, J.L., 1984. Estimating absorbed photosynthetic radiation and leaf area index from spectral reflectance in Wheat1. Agron. J. 76, 300–306.
Bechtold, S., Höfle, B., 2016. Helios: a multi-purpose LiDAR simulation framework for research, planning and training of laser scanning operations with airborne, ground-based mobile and stationary platforms. ISPRS Ann. Photogramm. Remote Sens. Spatial Inf. Sci. III-3, 161–168.
Béland, M., Widlowski, J.-L., Fournier, R.A., Côté, J.-F., Verstraete, M.M., 2011. Estimating leaf area distribution in savanna trees from terrestrial LiDAR measurements. Agric. For. Meteorol. 151, 1252–1266.
Béland, M., Baldocchi, D.D., Widlowski, J.-L., Fournier, R.A., Verstraete, M.M., 2014. On seeing the wood from the leaves and the role of voxel size in determining leaf area distribution of forests with terrestrial LiDAR. Agric. For. Meteorol. 184, 82–97.
Belgiu, M., Drăguţ, L., 2016. Random forest in remote sensing: a review of applications and future directions. ISPRS J. Photogramm. Remote Sens. 114, 24–31.
Bonan, G., 1995. Land-atmosphere interactions for climate system models: coupling biophysical, biogeochemical, and ecosystem dynamical processes. Remote Sens. Environ. 51, 57–73.
Bonan, G., 2015. Ecological Climatology: Concepts and Applications. Cambridge University Press.
Bouvier, M., Durrieu, S., Fournier, R.A., Renaud, J.-P., 2015. Generalizing predictive models of forest inventory attributes using an area-based approach with airborne LiDAR data. Remote Sens. Environ. 156, 322–334.
Calders, K., Origo, N., Disney, M., Nightingale, J., Woodgate, W., Armston, J., Lewis, P., 2018. Variability and bias in active and passive ground-based measurements of effective plant, wood and leaf area index. Agric. For. Meteorol. 252, 231–240.
Campbell, G.S., 1986. Extinction coefficients for radiation in plant canopies calculated using an ellipsoidal inclination angle distribution. Agric. For. Meteorol. 36, 317–321.
Campbell, G.S., 1990. Derivation of an angle density function for canopies with ellipsoidal leaf angle distributions. Agric. For. Meteorol. 49, 173–176.
Cattanio, J.H., 2017. Leaf area index and root biomass variation at different secondary forest ages in the eastern Amazon. For. Ecol. Manag. 400, 1–11.
Chen, J.M., 1996. Optically-based methods for measuring seasonal variation of leaf area index in boreal conifer stands. Agric. For. Meteorol. 80, 135–163.
Chen, J.M., Black, T., 1992. Defining leaf area index for non-flat leaves. Plant Cell Environ. 15, 421–429.
Chen, J.M., Cihlar, J., 1995. Quantifying the effect of canopy architecture on optical measurements of leaf area index using two gap size analysis methods. IEEE Trans. Geosci. Remote Sens. 33, 777–787.
Chen, J.M., Cihlar, J., 1996. Retrieving leaf area index of boreal conifer forests using Landsat TM images. Remote Sens. Environ. 55, 153–162.
Criminisi, A., Shotton, J., Konukoglu, E.J.F., Graphics, T.i.C., & Vision, 2012. Decision Forests: A Unified Framework for Classification, Regression, Density Estimation, Manifold Learning and Semi-Supervised Learning. 7. pp. 81–227.
Cutler, A., Cutler, D.R., Stevens, J.R., 2012. Random forests. In: In Ensemble machine learning. Springer, Boston, MA, pp. 157–175.
Demantke, J., Mallet, C., David, N., Vallet, B., 2011. Dimensionality based scale selection in 3D lidar point clouds. Int. Arch. Photogramm. Remote. Sens. Spat. Inf. Sci. 38, W12.
Farid, A., Goodrich, D.C., Bryant, R., Sorooshian, S., 2008. Using airborne lidar to predict leaf area index in cottonwood trees and refine riparian water-use estimates. J. Arid Environ. 72, 1–15.
Gleason, C.J., Im, J., 2012. Forest biomass estimation from airborne LiDAR data using machine learning approaches. Remote Sens. Environ. 125, 80–91.
Gobron, N., Pinty, B., Verstraete, M.M., 1997. Theoretical limits to the estimation of the leaf area index on the basis of visible and near-infrared remote sensing data. IEEE Trans. Geosci. Remote Sens. 35, 1438–1445.
Guan, H., Li, J., Chapman, M., Deng, F., Ji, Z., Yang, X., 2013. Integration of orthoimagery and lidar data for object-based urban thematic mapping using random forests. Int. J. Remote Sens. 34, 5166–5186.
Hancock, S., Essery, R., Reid, T., Carle, J., Baxter, R., Rutter, N., Huntley, B., 2014. Characterising forest gap fraction with terrestrial lidar and photography: an examination of relative limitations. Agric. For. Meteorol. 189–190, 105–114.
Hancock, S., Anderson, K., Disney, M., Gaston, K.J., 2017. Measurement of fine-spatial-resolution 3D vegetation structure with airborne waveform lidar: calibration and validation with voxelised terrestrial lidar. Remote Sens. Environ. 188, 37–50.
Hardwick, S.R., Toumi, R., Pfeifer, M., Turner, E.C., Nilus, R., Ewers, R.M., 2015. The relationship between leaf area index and microclimate in tropical forest and oil palm plantation: Forest disturbance drives changes in microclimate. Agric. For. Meteorol. 201, 187–195.
Heurich, M., Beudert, B., Rall, H., Křenová, Z., 2010. National parks as model regions for interdisciplinary long-term ecological research: The bavarian forest and šumavá national parks underway to transboundary ecosystem research. In: Müller, F., Baessler, C., Schubert, H., Klotz, S. (Eds.), Long-Term Ecological Research: Between Theory and Application. Springer Netherlands, Dordrecht, pp. 327–344.
Hill, R.A., Broughton, R.K., 2009. Mapping the understorey of deciduous woodland from leaf-on and leaf-off airborne LiDAR data: a case study in lowland Britain. ISPRS J. Photogramm. Remote Sens. 64, 223–233.
Hopkinson, C., Chasmer, L., 2009. Testing LiDAR models of fractional cover across multiple forest ecozones. Remote Sens. Environ. 113, 275–288.
Hopkinson, C., Lovell, J., Chasmer, L., Jupp, D., Kljun, N., van Gorsel, E., 2013. Integrating terrestrial and airborne lidar to calibrate a 3D canopy model of effective leaf area index. Remote Sens. Environ. 136, 301–314.
Hosoi, F., Omasa, K., 2006. Voxel-based 3-D modeling of individual trees for estimating leaf area density using high-resolution portable scanning Lidar. IEEE Trans. Geosci. Remote Sens. 44, 3610–3618.
Jensen, J.L.R., Humes, K.S., Vierling, L.A., Hudak, A.T., 2008. Discrete return lidar-based prediction of leaf area index in two conifer forests. Remote Sens. Environ. 112, 3947–3957.
Jonckheere, I., Fleck, S., Nackaerts, K., Muys, B., Coppin, P., Weiss, M., Baret, F., 2004. Review of methods for in situ leaf area index determination: part I. theories, sensors and hemispherical photography. Agric. For. Meteorol. 121, 19–35.
Kashani, A.G., Olsen, M.J., Parrish, C.E., Wilson, N., 2015. A review of LIDAR radiometric processing: from ad hoc intensity correction to rigorous radiometric calibration. 15, 28099–28128.
Kim, S., McGaughey, R.J., Andersen, H.-E., Schreuder, G., 2009. Tree species differentiation using intensity data derived from leaf-on and leaf-off airborne laser scanner data. Remote Sens. Environ. 113, 1575–1586.
Koenig, K., Höfle, B., Hämmerle, M., Jarmer, T., Siegmann, B., Lilienthal, H., 2015. Comparative classification analysis of post-harvest growth detection from terrestrial LiDAR point clouds in precision agriculture. ISPRS J. Photogramm. Remote Sens. 104, 112–125.
Korhonen, L., Korpela, I., Heiskanen, J., Maltamo, M., 2011. Airborne discrete-return LIDAR data in the estimation of vertical canopy cover, angular canopy closure and leaf area index. Remote Sens. Environ. 115, 1065–1080.
Leblanc, S.G., Chen, J.M., Kwong, M., 2002. Tracing radiation and architecture of canopies. In: TRAC Manual, (Version, 2).
Li, Y., Guo, Q., Tao, S., Zheng, G., Zhao, K., Xue, B., Su, Y., 2016. Derivation, validation, and sensitivity analysis of terrestrial laser scanning-based leaf area index. Can. J. Remote. Sens. 42, 719–729.
Li, Y., Guo, Q., Su, Y., Tao, S., Zhao, K., Xu, G., 2017. Retrieving the gap fraction, element clumping index, and leaf area index of individual trees using single-scan data from a terrestrial laser scanner. ISPRS J. Photogramm. Remote Sens. 130, 308–316.
Li, Z., Strahler, A., Schaaf, C., Jupp, D., Schaefer, M., Olofsson, P., 2018. Seasonal change of leaf and woody area profiles in a midlatitude deciduous forest canopy from classified dual-wavelength terrestrial lidar point clouds. Agric. For. Meteorol. 262, 279–297.
Liu, J., Skidmore, A.K., Wang, T., Zhu, X., Premier, J., Heurich, M., Beudert, B., Jones, S., 2019. Variation of leaf angle distribution quantified by terrestrial LiDAR in natural European beech forest. ISPRS J. Photogramm. Remote Sens. 148, 208–220.
Lovell, J., Jupp, D., van Gorsel, E., Jimenez-Berni, J., Hopkinson, C., Chasmer, L., 2011. Foliage profiles from ground based waveform and discrete point lidar. In: Proceedings of the SilviLaser 2011 Conference. Oct. 16–20, Hobart, Tasmania. Citeseer.
Luo, S., Wang, C., Pan, F., Xi, X., Li, G., Nie, S., Xia, S., 2015. Estimation of wetland vegetation height and leaf area index using airborne laser scanning data. Ecol. Indic. 48, 550–559.
Luo, S.Z., Chen, J.M., Wang, C., Gonsamo, A., Xi, X.H., Lin, Y., Qian, M.J., Peng, D.L., Nie, S., Qin, H.M., 2018. Comparative performances of airborne LiDAR height and intensity data for leaf area index estimation. IEEE Journal of Selected Topics in Applied Earth Observations and Remote Sensing 11, 300–310.
Ma, L., Zheng, G., Eitel, J.U.H., Magney, T.S., Moskal, L.M., 2016a. Determining woody-to-total area ratio using terrestrial laser scanning (TLS). Agric. For. Meteorol. 228, 217–228.
Ma, L., Zheng, G., Eitel, J.U.H., Moskal, L.M., He, W., Huang, H., 2016b. Improved salient feature-based approach for automatically separating photosynthetic and non-photosynthetic components within terrestrial lidar point cloud data of forest canopies. IEEE Trans. Geosci. Remote Sens. 54, 679–696.
Ma, L., Zheng, G., Eitel, J.U.H., Magney, T.S., Moskal, L.M., 2017. Retrieving forest canopy extinction coefficient from terrestrial and airborne lidar. Agric. For. Meteorol.

236, 1–21.
McGaughey, R.J., 2009. FUSION/LDV: Software for LIDAR Data Analysis and Visualization. 123.
Moorthy, I., Miller, J.R., Hu, B., Chen, J., Li, Q., 2008. Retrieving crown leaf area index from an individual tree using ground-based lidar data. Can. J. Remote. Sens. 34, 320–332.
Næsset, E., 2005. Assessing sensor effects and effects of leaf-off and leaf-on canopy conditions on biophysical stand properties derived from small-footprint airborne laser data. Remote Sens. Environ. 98, 356–370.
Næsset, E., Bjerknes, K.-O., 2001. Estimating tree heights and number of stems in young forest stands using airborne laser scanner data. Remote Sens. Environ. 78, 328–340.
Neumann, H., Den Hartog, G., Shaw, R.J.A., Meteorology, F, 1989. Leaf area measurements based on hemispheric photographs and leaf-litter collection in a deciduous forest during autumn leaf-fall. 45, 325–345.
Nilson, T., 1971. A theoretical analysis of the frequency of gaps in plant stands. Agric. Meteorol. 8, 25–38.
Nilsson, A., 2016. Effect of Continuity, Area, Connectivity and Surrounding Landscape on Forest Specialist Plant Species in Deciduous Forest.
Norden, B., Rørstad, P.K., Löf, M., Rusch, G.M., 2018. Potential for restoration of temperate deciduous forest by thinning of mixed forests on abandoned agricultural land. In: ECCB2018: 5th European Congress of Conservation Biology. Open Science Centre, University of Jyväskylä, Jyväskylä, Finland *12th-15th of June 2018*.
Oshio, H., Asawa, T., Hoyano, A., Miyasaka, S., 2015. Estimation of the leaf area density distribution of individual trees using high-resolution and multi-return airborne LiDAR data. Remote Sens. Environ. 166, 116–125.
Parent, J.R., Volin, J.C., 2014. Assessing the potential for leaf-off LiDAR data to model canopy closure in temperate deciduous forests. ISPRS J. Photogramm. Remote Sens. 95, 134–145.
Pearse, G.D., Morgenroth, J., Watt, M.S., Dash, J.P., 2017. Optimising prediction of forest leaf area index from discrete airborne lidar. Remote Sens. Environ. 200, 220–239.
Pettorelli, N., Wegmann, M., Skidmore, A., Mücher, S., Dawson, T.P., Fernandez, M., Lucas, R., Schaepman, M.E., Wang, T., O'Connor, B., Jongman, R.H.G., Kempeneers, P., Sonnenschein, R., Leidner, A.K., Böhm, M., He, K.S., Nagendra, H., Dubois, G., Fatoyinbo, T., Hansen, M.C., Paganini, M., de Klerk, H.M., Asner, G.P., Kerr, J.T., Estes, A.B., Schmeller, D.S., Heiden, U., Rocchini, D., Pereira, H.M., Turak, E., Fernandez, N., Lausch, A., Cho, M.A., Alcaraz-Segura, D., McGeoch, M.A., Turner, W., Mueller, A., St-Louis, V., Penner, J., Vihervaara, P., Belward, A., Reyers, B., Geller, G.N., 2016. Framing the concept of satellite remote sensing essential biodiversity variables: challenges and future directions. Remote Sensing in Ecology and Conservation 2, 122–131.
Pfennigbauer, M., Ullrich, A., 2010. Improving quality of laser scanning data acquisition through calibrated amplitude and pulse deviation measurement. In: Proc. SPIE 7684, Laser Radar Technology and Applications XV, pp. 76841F.
Picard, R.R., Cook, R.D., 1984. Cross-validation of regression models. J. Am. Stat. Assoc. 79, 575–583.
Pisek, J., Sonnentag, O., Richardson, A.D., Mõttus, M., 2013. Is the spherical leaf inclination angle distribution a valid assumption for temperate and boreal broadleaf tree species? Agric. For. Meteorol. 169, 186–194.
Rautiainen, M., 2005. Retrieval of leaf area index for a coniferous forest by inverting a forest reflectance model. Remote Sens. Environ. 99, 295–303.
Roy, S., Byrne, J., Pickering, C., 2012. A systematic quantitative review of urban tree benefits, costs, and assessment methods across cities in different climatic zones. Urban For. Urban Green. 11, 351–363.
Shi, Y., Wang, T., Skidmore, A.K., Heurich, M., 2018. Important LiDAR metrics for discriminating forest tree species in Central Europe. ISPRS J. Photogramm. Remote Sens. 137, 163–174.
Skidmore, A., Pettorelli, N., Coops, N., Geller, G., Hansen, M., Lucas, R., Mücher, C., O'Connor, B., Paganini, M., Pereira, H., 2015. Environmental science: agree on biodiversity metrics to track from space. Nature 523, 403.
Solberg, S., Brunner, A., Hanssen, K.H., Lange, H., Næsset, E., Rautiainen, M., Stenberg, P., 2009. Mapping LAI in a Norway spruce forest using airborne laser scanning. Remote Sens. Environ. 113, 2317–2327.
Sumnall, M., Fox, T.R., Wynne, R.H., Thomas, V.A., 2017. Mapping the height and spatial cover of features beneath the forest canopy at small-scales using airborne scanning discrete return Lidar. ISPRS J. Photogramm. Remote Sens. 133, 186–200.
Tang, H., Brolly, M., Zhao, F., Strahler, A.H., Schaaf, C.L., Ganguly, S., Zhang, G., Dubayah, R., 2014. Deriving and validating Leaf Area Index (LAI) at multiple spatial scales through lidar remote sensing: a case study in Sierra National Forest, CA. Remote Sens. Environ. 143, 131–141.
Tian, Y., Zheng, Y., Zheng, C., Xiao, H., Fan, W., Zou, S., Wu, B., Yao, Y., Zhang, A., Liu, J., 2015. Exploring scale-dependent ecohydrological responses in a large endorheic river basin through integrated surface water-groundwater modeling. 51, 4065–4085.
Tillack, A., Clasen, A., Kleinschmit, B., Förster, M., 2014. Estimation of the seasonal leaf area index in an alluvial forest using high-resolution satellite-based vegetation indices. Remote Sens. Environ. 141, 52–63.
Vauhkonen, J., Korpela, I., Maltamo, M., Tokola, T., 2010. Imputation of single-tree attributes using airborne laser scanning-based height, intensity, and alpha shape metrics. Remote Sens. Environ. 114, 1263–1276.
Véga, C., Renaud, J.P., Durrieu, S., Bouvier, M., 2016. On the interest of penetration depth, canopy area and volume metrics to improve Lidar-based models of forest parameters. Remote Sens. Envirobn. 175, 32–42.
Vicari, M.B., Disney, M., Wilkes, P., Burt, A., Calders, K., Woodgate, W., 2019. Leaf and wood classification framework for terrestrial LiDAR point clouds. Methods Ecol. Evol. 10, 680–694.
Vincent, G., Antin, C., Laurans, M., Heurtebize, J., Durrieu, S., Lavalley, C., Dauzat, J., 2017. Mapping plant area index of tropical evergreen forest by airborne laser scanning. A cross-validation study using LAI2200 optical sensor. Remote Sens. Environ. 198, 254–266.
Weber, J., Penn, J., 1995. Creation and rendering of realistic trees. In: Proceedings of the 22nd Annual Conference on Computer Graphics and Interactive Techniques. ACM, pp. 119–128.
Weiss, M., Baret, F., Smith, G., Jonckheere, I., Coppin, P., 2004. Review of methods for in situ leaf area index (LAI) determination: part II. Estimation of LAI, errors and sampling. Agric. For. Meteorol. 121, 37–53.
White, J.C., Arnett, J.T., Wulder, M.A., Tompalski, P., Coops, N.C., 2015. Evaluating the impact of leaf-on and leaf-off airborne laser scanning data on the estimation of forest inventory attributes with the area-based approach. Can. J. For. Res. 45, 1498–1513.
Wilson, J.W.J.A.j.o.b. (1963). Estimation of foliage denseness and foliage angle by inclined point quadrats, 11, 95–105.7
Xiao, Q., McPherson, E.G., 2002. Rainfall interception by Santa Monica's municipal urban forest. Urban Ecosyst. 6, 291–302.
Zhao, F., Yang, X., Schull, M.A., Román-Colón, M.O., Yao, T., Wang, Z., Zhang, Q., Jupp, D.L.B., Lovell, J.L., Culvenor, D.S., Newnham, G.J., Richardson, A.D., Ni-Meister, W., Schaaf, C.L., Woodcock, C.E., Strahler, A.H., 2011. Measuring effective leaf area index, foliage profile, and stand height in New England forest stands using a full-waveform ground-based lidar. Remote Sens. Environ. 115, 2954–2964.
Zheng, G., Ma, L.X., He, W., Eitel, J.U.H., Moskal, L.M., Zhang, Z.Y., 2016. Assessing the contribution of woody materials to Forest angular gap fraction and effective leaf area index using terrestrial laser scanning data. IEEE Trans. Geosci. Remote Sens. 54, 1475–1487.
Zhu, X., Skidmore, A.K., Darvishzadeh, R., Niemann, K.O., Liu, J., Shi, Y., Wang, T., 2018. Foliar and woody materials discriminated using terrestrial LiDAR in a mixed natural forest. Int. J. Appl. Earth Obs. Geoinf. 64, 43–50.